0026-895X/07/7201-121–131$20.00
MOLECULAR PHARMACOLOGY
Vol. 72, No. 1
34140/3224219

Mol Pharmacol 72:121–131, 2007
Printed in U.S.A.

Site-Specific Inhibition of Glomerulonephritis Progression by Targeted Delivery of Dexamethasone to Glomerular Endothelium

Sigridur A. Ásgeirsdóttir, Jan A. A. M. Kamps, Hester I. Bakker, Peter J. Zwiers, Peter Heeringa, Karen van der Weide, Harry van Goor, Arjen H. Petersen, Henriëtte Morselt, Henk E. Moorlag, E. Steenbergen, Cees G. Kallenberg, and Grietje Molema

Medical Biology Section (S.A.Á., J.A.A.M.K., H.I.B., P.J.Z., P.H., K.v.d.W., A.H.P., H.M., H.E.M., G.M.) and Pathology Section (H.v.G.), Department of Pathology & Laboratory Medicine, University Medical Center Groningen, University of Groningen, The Netherlands; Department of Pathology, Radboud University Nijmegen Medical Centre, Nijmegen, The Netherlands (E.S.); and Department of Clinical Immunology, University Medical Center Groningen, University of Groningen, The Netherlands (C.G.K.)

Received January 15, 2007; accepted April 23, 2007

ABSTRACT

Glomerulonephritis represents a group of renal diseases with glomerular inflammation as a common pathologic finding. Because of the underlying immunologic character of these disorders, they are frequently treated with glucocorticoids and cytotoxic immunosuppressive agents. Although effective, use of these compounds has limitations as a result of toxicity and systemic side effects. In the current study, we tested the hypothesis that targeted delivery of dexamethasone (dexa) by immunoliposomes to activated glomerular endothelium decreases renal injury but prevents its systemic side effects. E-selectin was chosen as a target molecule based on its disease-specific expression on activated glomerular endothelium in a mouse anti-glomerular basement membrane glomerulonephritis. Site-selective delivery of Ab_{Esel} liposome–encapsulated dexamethasone strongly reduced glomerular proinflammatory gene expression without affecting blood glucose levels, a severe side effect of administration of free dexamethasone. Dexa-Ab_{Esel} liposomes reduced renal injury as shown by a reduction of blood urea nitrogen levels, decreased glomerular crescent formation, and down-regulation of disease-associated genes. Immunoliposomal drug delivery to glomerular endothelium presents a powerful new strategy for treatment of glomerulonephritis to sustain efficacy and prevent side effects of potent anti-inflammatory drugs.

The glomerulonephritides comprise a spectrum of inflammatory diseases specifically affecting the glomeruli (Eremina et al., 2003). In general, glomerular inflammation is characterized by activation of various common proinflammatory pathways, including complement activation, production of pro-inflammatory cytokines, endothelial activation, and influx of circulating leukocytes (Falk et al., 2004). As a consequence, glomerular injury and proteinuria develop.

Based on the underlying immunologic nature of glomerulonephritides, these disorders are frequently treated with glucocorticosteroids in combination with cytotoxic agents (Javaid and Quigg, 2005). Glucocorticosteroids and cytotoxic agents, such as cyclophosphamide, are potent anti-inflammatory and immunosuppressive agents but have their limitations with regard to toxicity and side effects (Chadban and Atkins, 2005; Tam, 2006). Identifying more effective and less toxic treatment for glomerulonephritis still remains a major aim. One way to increase drug efficacy and decrease side effects of treatment is to selectively deliver the therapeutic entity into the diseased tissue. Endothelial cells have obtained considerable attention as targets for this purpose (Kamps et al., 1997; Ulbrich et al., 2003; Kuldo et al., 2005). Not only are endothelial cells in direct contact with the blood stream and consequently accessible for systemically administered therapeutics but also they play an essential role in

This work was supported by grants C01.1988 and C04.2080 from the Dutch Kidney Foundation.
Article, publication date, and citation information can be found at http://molpharm.aspetjournals.org.
doi:10.1124/mol.107.034140.

ABBREVIATIONS: VCAM, vascular cell adhesion molecule; ICAM, intercellular adhesion molecule; Ab_{Esel}, anti E-selectin antibody; TNF, tumor necrosis factor; PBS, phosphate-buffered saline; PAS, periodic acid-Schiff base; BUN, blood urea nitrogen; RT, reverse transcription; PCR, polymerase chain reaction; GBM, glomerular basement membrane; TGF, transforming growth factor; MCP1, monocyte chemoattractant protein-1; IL, interleukin; Dexa, dexamethasone.

the pathological process associated with glomerulonephritis. The interaction of leukocytes with activated endothelial cells is well orchestrated via processes of tethering and rolling, mediated by endothelial expression of P- and E-selectin, followed by firm adhesion through interaction between integrins of the leukocytes, and endothelial members of the immunoglobulin superfamily, including VCAM-1 and ICAM-1 (Vestweber, 2002).

Liposomes are high-capacity drug carriers that, when modified with monoclonal antibodies, can be targeted to a selective target epitope of choice (Spragg et al., 1997; Kamps and Molema, 2006). Inflammation-related cell-adhesion molecules, including E-selectin and VCAM-1, are attractive candidates as target epitopes on activated endothelium because of their increased expression during inflammation and their predominant endothelial location.

The current study was designed to explore the feasibility of local immunoliposomal delivery of the glucocorticosteroid dexamethasone into activated glomerular endothelium in glomerulonephritis.

Materials and Methods

Preparation of Immunoliposomes. Synthesis of immunoliposomes was as described previously (Kamps et al., 1996; Bartsch et al., 2005). In short, lipids from stock solutions of 1-palmitoyl-2-oleoyl-*sn*-glycero-3-phosphocholine, cholesterol, 1,2-distearoyl-*sn*-glycero-3-phosphoethanolamine-*N*-[methoxy(polyethylene glycol)-2000] and 1,2-distearoyl-*sn*-glycero-3-phosphoethanolamine-*N*-[methoxy(polyethylene glycol)-2000]-maleimide in chloroform/methanol (9:1), were mixed in a molar ratio of 55:40:4:1, dried under reduced nitrogen pressure, dissolved in cyclohexane, and lyophilized. The lipids were then hydrated in 10 mM HEPES and 135 mM NaCl, pH 6.7, or, when appropriate, in an aqueous solution of 75 to 100 mg/ml dexamethasone disodium phosphate. The liposomes formed were sized by repeated extrusion (13 times) through polycarbonate filters (Costar; Corning Life Sciences, Acton, MA), pore size 50 nm, using a high-pressure extruder (Lipex, Vancouver, BC, Canada). The monoclonal rat anti-mouse E-selectin antibody, (MES-1, kindly provided by Dr. D. Brown, UCB Celltech, Slough, UK) and irrelevant rat IgG (Sigma-Aldrich Chemie, Zwijndrecht, The Netherlands) were thiolated by means of *N*-succinimidyl-*S*-acetylthioacetate and coupled to a maleimide group at the distal end of the polyethylene glycol chain by a sulfhydryl-maleimide coupling technique. The immunoliposomes were characterized by determining protein content, using mouse IgG as a standard (Peterson, 1977), and phospholipid phosphorus content (Bottcher et al., 1961). Total liposomal lipid concentrations were adjusted for the amount of cholesterol present in the liposome preparations. Anti-E-selectin antibody (52.1 ± 25.6 g/mol of lipid) and irrelevant rat IgG (53.6 ± 23.1 g/mol of lipid) was coupled. Particle size was analyzed by dynamic light scattering using a Nicomp model 370 submicron particle analyzer (Santa Barbara, CA) in the volume weighing model. The diameter of Ab_{Esel} liposomes was 114.0 ± 31.1 nm and that of IgG liposomes 103.3 ± 16.4 nm. The number of antibody molecules coupled per liposome was calculated based on the measured concentration (C_{Ab}) of antibody (grams per mol of lipid) and diameter (nanometers) of the immunoliposomes (R) and the assumption that the liposomes were approximately spherical. From this, and literature values for specific lipid volume (V_{Ls}) of 1.25 nm^3, liposome bilayer thickness (d_{bl}) of 3.7 nm (Enoch and Strittmatter, 1979), and the molecular mass of the antibody molecule (M_{Ab}) of 150 kDa, the number of antibodies coupled to the liposomes was estimated to be 20 Ab_{Esel} molecules per liposome and 17 IgG molecules per liposome by geometric arguments according to the following formula: $\pi/6 \times C_{Ab} \times (3d_{bl} \times R^2 - 3R \times {d_{bl}}^2 + {d_{bl}}^3) \times {M_{Ab}}^{-1} \times {V_{Ls}}^{-1}$ (Adrian et al., 2007). The content of encapsulated dexamethasone disodium-phosphate (Bufa, Hilversum, The Netherlands) was determined after Bligh and Dyer extraction in the resulting methanol/H_2O phase by high-performance liquid chromatography (Melgert et al., 2000). Dexamethasone (55.4 ± 6.5 $\mu g/\mu mol$ of lipid) was encapsulated.

Animals. C57bl/6 female mice were purchased from Harlan (Zeist, The Netherlands). Animals were maintained on mouse chow and tap water ad libitum in a temperature-controlled chamber at 24°C with a 12-h light/dark cycle. All animal experiments were performed upon approval of the local Animal Care and Use Committee of Groningen University. After an adaptation period of 1 week, mice were allocated to the experiments as described below.

Induction of Accelerated Anti-GBM Glomerulonephritis. The IgG fraction was isolated from polyclonal sheep anti-mouse glomerular basement membrane (GBM) serum by HiTrap Sephadex-Protein G column (GE Healthcare Europe GmbH, Diegem, Belgium). Induction of anti-GBM glomerulonephritis was modified from the earlier described protocol (Assmann et al., 1985; Heeringa et al., 2000). In short, immunization was initiated by 100 μl (2 mg/ml) commercially available sheep IgG (Sigma-Aldrich Chemie) mixed with 100 μl of complete Freund's adjuvant (BD PharMingen, Alphen aan den Rijn, The Netherlands), and injected i.p. After 6.5 days, glomerulonephritis was induced by i.v. injection with 1 mg of sheep anti-mouse GBM antibodies and 200 ng of recombinant mouse tumor necrosis factor α (TNFα; BioSource Europe, Nivelles, Belgium). The total volume injected was 200 μl. Mice were sacrificed at 2 h ($n = 12$), 24 h ($n = 6$), 48 h ($n = 9$), 7 days ($n = 5$), and 14 days ($n = 11$). Organs were perfused with ice-cold phosphate-buffered saline (PBS) and harvested. One kidney was fixed in 4% formaldehyde/PBS and embedded in paraffin for morphological analysis, the other kidney, liver, spleen, and heart were snap-frozen in liquid nitrogen and stored at −80°C.

Glomerulonephritis Development and Disease Progression. Five-micrometer cryosections were fixed in acetone for 10 min and incubated with fluorescein isothiocyanate-labeled rabbit anti-sheep IgG or -anti-mouse IgG antibodies (DakoCytomation Denmark A/S, Glostrup, Denmark). Nuclear counterstaining was performed with 4′,6-diamidino-2-phenylindole (Roche Diagnostics Nederland BV, Almere, The Netherlands). Sections were examined using a fluorescence microscope (DM RXA; Leica, Cambridge, UK) and Leica Q600 Qwin V01.06 software.

For morphological analysis of renal injury, formaldehyde-fixed, paraffin-embedded 4-μm sections were stained with periodic acid-Schiff base (PAS). The amount of PAS-positive material within glomeruli was semiquantitatively scored as described previously (Heeringa et al., 2000). A glomerular crescent score was determined for each animal. Only glomeruli that had two or more layers of cells in Bowman's space were considered crescent. The presence of PAS-

TABLE 1
Primers and probes used for quantitative RT-PCR

E-selectin	
Forward	CAACGTCTAGGTTCAAAACAATCAG
Probe	CACAAATGCATCGTGGGA
Reverse	TTAAGCAGGCAAGAGGAACCA
VCAM-1	
Forward	TGAAGTTGGCTCACAATTAAGAAGTT
Probe	AACACTTGATGTAAAAGGA
Reverse	TGCGCAGTAGAGTGCAAGGA
ICAM-1	
Forward	ATGGGAATGTCACCAGGAATG
Probe	CAGTACTGTACCACTCTC
Reverse	GCACCAGAATGATTATAGTCCAGTTATT
P-selectin	Mm00441295_m1 (Applied Biosystems)
TNFα	Mm00443258_m1 (Applied Biosystems)
IL-1β	Mm00434228_m1 (Applied Biosystems)
IL-6	Mm00446190_m1 (Applied Biosystems)
MCP1	Mm00441242_m1 (Applied Biosystems)
TGFβ	Mm00441724_m1 (Applied Biosystems)
GAPDH	Mm99999915_g1 (Applied Biosystems)

positive material and glomerular crescent was expressed as mean scores obtained by two experimentally blinded observers counting between 50 and 100 glomeruli per kidney section.

Homing Studies and Pharmacological Effects of Targeted Delivery of Dexamethasone versus Free Dexamethasone. For homing studies and acute pharmacological effects, dexamethasone (Genfarma, Maarsen, The Netherlands; 25 μg per mouse; $n = 7$), Ab_{Esel} liposomes (0.4 μmol of lipid; $n = 4$), IgG liposomes (0.4 μmol of lipid; $n = 3$), and Dexa-Ab_{Esel} liposomes (0.4 μmol of lipid, 25 μg of dexamethasone phosphate; $n = 6$), respectively, were i.v. injected at the onset of glomerulonephritis induction. To analyze pharmacological effects at day 14, mice ($n = 6$ per treatment) were i.v. injected twice with Ab_{Esel} liposomes, Dexa-Ab_{Esel} liposomes, Dexa-IgG liposomes, and free dexamethasone, at the onset of glomerulonephritis induction and at day 7 (dosages as above). In the group treated with empty Ab_{Esel} liposomes, one mouse lost more than 15% body weight and was taken out of the experiment at day 4.

Blood and Urine Examinations. Blood urea nitrogen (BUN) was measured in plasma collected at the time of sacrifice by an enzymatic degradation assay on a Vitros 250 automated analyzer (Johnson & Johnson, South Brunswick, NJ). Glucose concentration was determined in plasma using a glucose oxidase analyzer (2300 STAT; YSI Inc., Yellow Springs, OH). For collection of urine, mice were placed for 24 h in individual metabolic cages. Urinary albumin content was measured in 96-well microplates (Nalge Nunc International, Rochester, NY) with the mouse albumin enzyme-linked immunosorbent assay quantitation kit (Bethyl Laboratories, Montgomery, TX) using purified mouse albumin as a reference. Plasma and

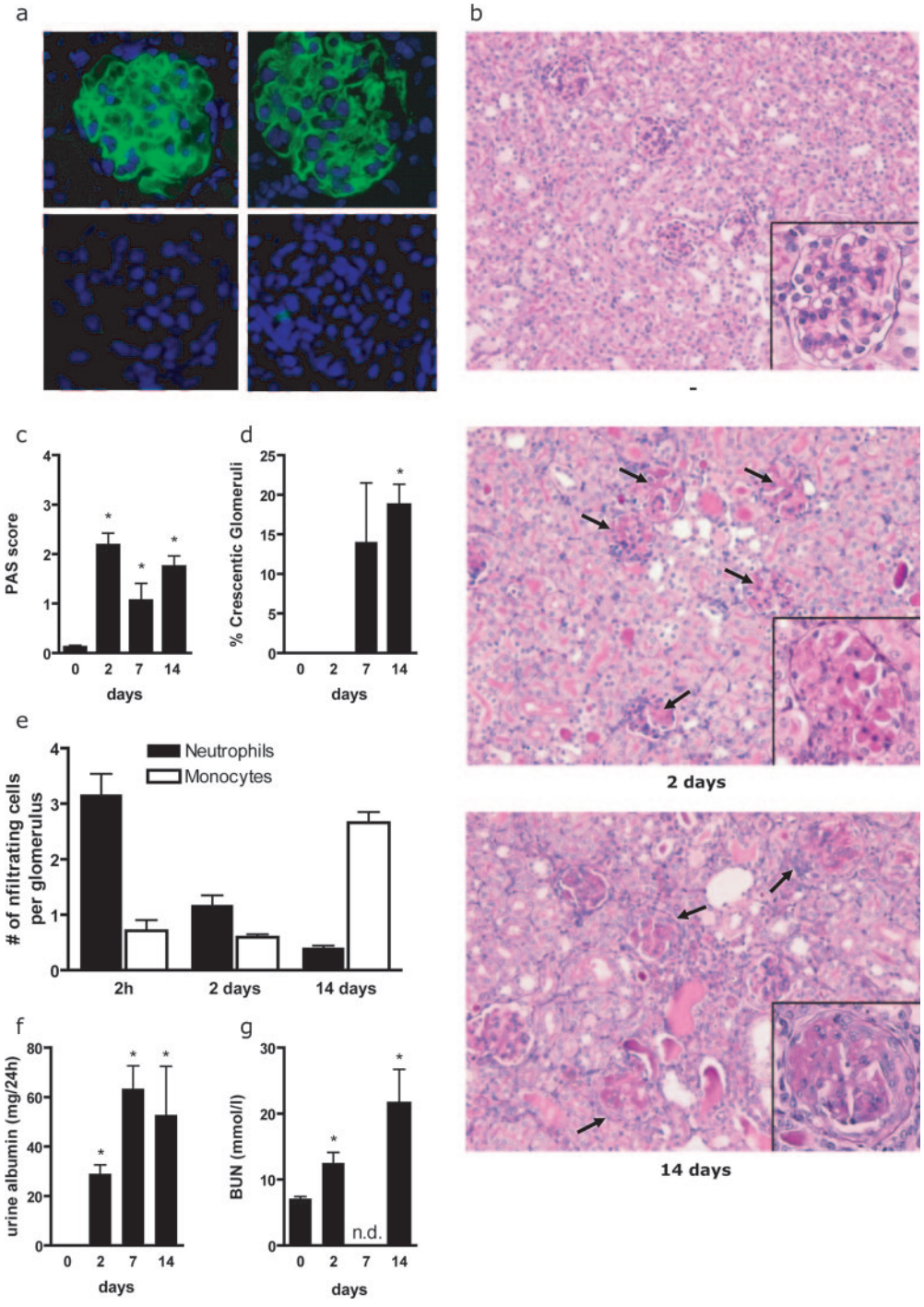

Fig. 1. Development of glomerulonephritis. a, glomerular deposition of sheep (left) and mouse (right) immunoglobulin at 1 day after glomerulonephritis induction (top). Immunofluorescent staining along the glomerular capillary wall was observed at all time points from 2 h until 14 days. No staining was observed in healthy control mice (bottom). Nuclear counterstaining was performed with 4′,6-diamidino-2-phenylindole. b, light microscopy (PAS stain) of kidney from untreated mouse (top), and mice sacrificed 2 (middle) and 14 days (bottom) after induction of glomerulonephritis. Arrows indicate glomerular thrombus formation at day 2 and crescent formation at day 14. Insets indicate a normal glomerulus with open capillaries and Bowman capsule (top), PAS-positive glomerulus with intracapillary thrombus (middle), and glomerular crescent formation (bottom). c, semiquantitative scoring of glomerular deposits of PAS-positive material as a measure of glomerular injury. d, presence of glomerular crescents was observed at 7 and 14 days after glomerulonephritis induction. e, glomerular infiltration of neutrophils and monocytes. f, development of albuminuria after induction of glomerulonephritis. g, BUN levels after induction of glomerulonephritis. BUN levels were not determined (n.d.) at day 7. Data in c–g are presented as mean values ± S.E.M. of 5–12 animals per treatment. *, $p < 0.05$ compared with healthy control mice in c, d, f, and g.

urinary creatinine levels were measured by enzymatic colorimetric method using Creatinine plus (Roche, Woerden, The Netherlands), which allows precise and specific quantification of creatinine (Keppler et al., 2007). The creatinine clearance (C_{Cr}) was calculated according to the formula $C_{Cr} = [Cr_{urine}] \times V_{olume\ urine} \times [Cr_{plasma}]^{-1}$. Urine volume was measured in milliliters per minute.

Quantitative Gene Expression Analysis by Real-Time RT-PCR. Total RNA was isolated from 10 8-μm cryosections with RNeasy mini kit (QIAGEN Benelux B.V., Venlo, The Netherlands) including a DNase treatment on the column. RNA integrity was studied by gel electrophoresis and RNA yield (OD_{260}) and purity (OD_{260}/OD_{280}) were measured by ND-1000 UV-Vis Spectrophotometer (NanoDrop Technologies, Rockland, DE). One microgram of RNA was reverse-transcribed using SuperScript III reverse transcriptase (Invitrogen, Breda, The Netherlands) and random hexamer primers (Promega, Leiden, The Netherlands). Quantitative PCR amplifications were performed according to manufacturers protocol on an ABI Prism 7900HT Sequence Detection System (Applied Biosystems, Applera Nederland, Nieuwerkerk a/d IJssel, The Netherlands). Primers and probes for E-selectin, VCAM-1, and ICAM-1 were purchased as customized assays from Applied Biosystems. These primer/probes span multiple exons and were designed according to the same quality criteria as the Assays-on-Demand primer/probes used. Sequences and accession numbers are shown in Table 1. All PCR reactions were carried out in triplicate. Relative quantitation of gene expression was calculated based on the comparative cycle threshold (C_t) method ($\Delta Ct = Ct_{gene\ of\ interest} - Ct_{housekeeping\ gene}$). Comparison of gene expressions in different samples was performed based on the differences in ΔCt of individual samples ($\Delta\Delta Ct$).

TABLE 2

mRNA levels of proinflammatory genes in kidney of healthy control mice based on the number of cycles necessary for a fixed threshold value (C_t) in quantitative RT-PCR

Values represent mean $C_t \pm$ S.D., $n = 3$. Higher C_t value represents lower expression level. One C_t value difference = 2-fold expression level difference.

GAPDH (housekeeping gene)	19.4 ± 0.5
P-selectin	33.0 ± 0.6
E-selectin	31.3 ± 0.6
VCAM-1	27.5 ± 0.5
ICAM-1	27.3 ± 0.5
TNFα	31.9 ± 0.5
IL-1β	32.5 ± 0.7
MCP1	32.0 ± 0.4
TGFβ	26.3 ± 0.6

Immunohistochemical Analysis of Cell Adhesion Molecules, Immune Cell Infiltrates, and Localization of Immunoliposomes. Five-micrometer cryosections were fixed in acetone for 10 min and incubated for 45 min with primary rat anti-mouse monoclonal antibodies: anti-E-selectin (MES-1), anti-VCAM-1 (clone M/K-2.7; American Type Culture Collection, Manassas VA) anti-neutrophil (NIMP-R14), and anti-monocyte/macrophage (FA-11). Endogenous biotin was blocked by Biotin Blocking System (DakoCytomation Denmark A/S), and peroxidase activity was blocked by incubation with 0.1% H_2O_2 in PBS for 10 min. Thereafter, sections were incubated for 1 h with biotin labeled rabbit anti-rat antibodies (dilution 1:300 in PBS; DakoCytomation Denmark A/S) in the presence of 5% normal mouse serum and 5% normal sheep serum and incubated for 30 min with Streptavidin-ABComplex-horseradish peroxidase (DakoCytomation Denmark A/S). Peroxidase activity was detected with 3-amino-9-ethylcarbazole (Sigma-Aldrich Chemie), and sections were counterstained with Mayer's hematoxylin (Klinipath, Duiven, The Netherlands). Isotype-matched controls were carried out for all primary antibodies and consistently found to be devoid of staining. Immunostaining of E-selectin in glomeruli was quantified by counting the number of glomerular cross-sections expressing E-selectin. Glomerular infiltrates were evaluated by counting the number of stained cells in glomeruli. Results were expressed as mean scores obtained by two experimentally blinded observers counting between 50 and 100 glomeruli per mouse.

To analyze accumulation of immunoliposomes in kidney, heart, liver, and spleen, immunohistochemical staining for i.v. injected liposomal anti-E-selectin antibodies was performed as described above, except for omitting incubation with primary antibody. For quantitative analysis of staining of immunoliposomes in glomeruli morphometric analysis of 50 glomeruli per mouse was carried out using Leica QWin image analysis software. Numbers represent percentage of stained area within glomeruli.

Laser Dissection Microscopy to Isolate Glomeruli. Five-micrometer cryosections were mounted on 1.35-μm polyethylene-naphthalene membranes attached to normal 1-mm slides (P.A.L.M. Microlaser Technologies GmbH, Bernried, Germany), fixed in acetone (3 min), and stained with Mayer's hematoxylin (2 min, 25 μl per section), washed with diethyl pyrocarbonate-treated water (10 s, 25 μl per section), and air-dried. Glomeruli were dissected using the Laser Robot Microbeam System (P.A.L.M. Microlaser Technology). Eight hundred dissected glomeruli were collected directly in RNA lysis buffer (Stratagene Europe, Amsterdam, The Netherlands) in

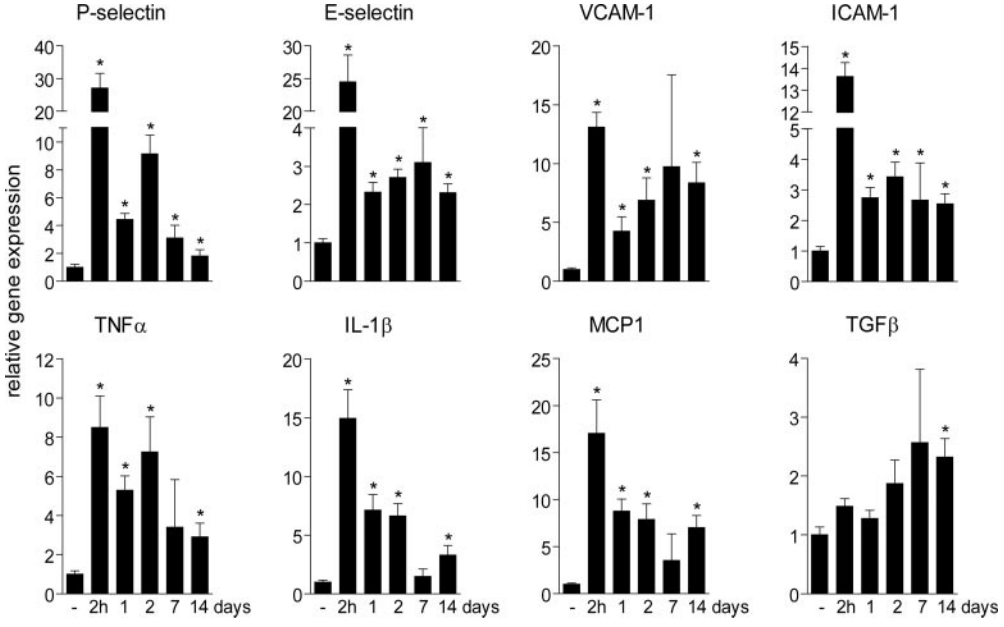

Fig. 2. Quantitative gene expression analysis of the cell adhesion molecules P- and E-selectin, VCAM-1, and ICAM-1, cytokines TNFα, IL-1β, IL-6, MCP1, and TGFβ in kidney of untreated mice (−), and at 2 h and 1, 2, 7, and 14 days after induction of glomerulonephritis. Expression levels of mRNA in untreated mice were arbitrarily set at 1. Data are presented as mean values ± S.E.M. of 5–12 animals per treatment. *, $p < 0.05$ compared with nontreated animals.

the cap of a microcentrifuge tube via laser pressure catapulting. Extraction of total RNA and DNase treatment were carried out according to the protocol of StrataPrep total RNA microprep kit (Stratagene). Quantitative RT-PCR was carried out as described above.

Statistical Analysis. Statistical significance of differences was studied by means of the two-sided Student's t test, assuming equal variances, except for semiquantitative scoring of PAS-positive material. In the latter, statistical significance of differences was calculated by Mann-Whitney nonparametric test. Differences were considered to be significant when $p < 0.05$

Results

Induction and Development of Glomerulonephritis. Injection of heterologous antibodies directed against GBM resulted in onset of glomerulonephritis in mice preimmunized with nonspecific sheep antibodies. We adapted the classic accelerated anti-GBM glomerulonephritis model (Assmann et al., 1985) by including TNFα in the anti-GBM antibody injection. This resulted in fast, reproducible, and progressive inflammation in the glomeruli, whereas TNFα or anti-GBM antibodies alone did not result in significant leukocyte influx or glomerular injury (data not shown). Figure 1 demonstrates the development of progressive glomerulonephritis in our model at different time points from 2 h to 2 weeks. Glomerular depositions of sheep and mouse immunoglobulin were observed at all time points (Fig. 1a) with formation of glomerular intracapillary PAS-positive thrombus starting at 2 days (Fig. 1, b and c). In addition, mild extracapillary proliferation and intratubular protein casts were noted, all indicative of glomerulonephritis induction (Fig. 1b). Glomerular accumulations of PAS-positive material were highest at 2 days and remained present for 14 days (Fig. 1c). Crescent formation was detected at 7 and 14 days after disease induction (Fig. 1, b and d). Two hours after glomerulonephritis induction, a peak of intraglomerular neutrophils was observed (Fig. 1e). The glomerular accumulation of neutrophils subsequently decreased in time, which was paralleled by an increase of intraglomerular monocytes (Fig. 1e), a time dependent pattern that is characteristic for the experimental anti-GBM glomerulonephritis model (Assmann et al., 1985; Masaki et al., 2003). Albuminuria was markedly increased after induction of glomerulonephritis to >50 mg per 24 h at days 7 and 14, whereas untreated mice secreted less than 0.1 mg of albumin per 24 h (Fig. 1f). At the same time, glomerular filtration function deteriorated (Fig. 1g).

To further examine the disease process, expression of proinflammatory genes was analyzed by quantitative RT-PCR. First, threshold C_t values in kidneys of untreated mice were determined. Expression of cytokines and P- and E-selectin was low, whereas VCAM-1, ICAM-1, and TGFβ were moderately expressed in healthy kidneys (Table 2). A rapid up-regulation of cell adhesion molecules and cytokines was observed 2 h after onset of glomerulonephritis (Fig. 2). The expression of cell adhesion molecules and cytokines was significantly higher compared with untreated animals throughout the experiment. Expression of the fibrosis related TGFβ enhanced slightly in time, indicative of ongoing glomerular injury and crescent formation (Border and Noble, 1994).

To characterize the proinflammatory gene expression profile specifically in glomeruli at the early stages of disease, we analyzed laser microdissected glomeruli. It is noteworthy that a spatial and temporal heterogenic regulation of proinflammatory genes in response to disease induction was observed. E-selectin was preferentially up-regulated in glomeruli at all time points (Fig. 3a). Initially P-selectin was more abundantly expressed in the glomeruli than in total kidney isolates, whereas up-regulation of VCAM-1 was more pronounced in the nonglomerular vascular compartments at all

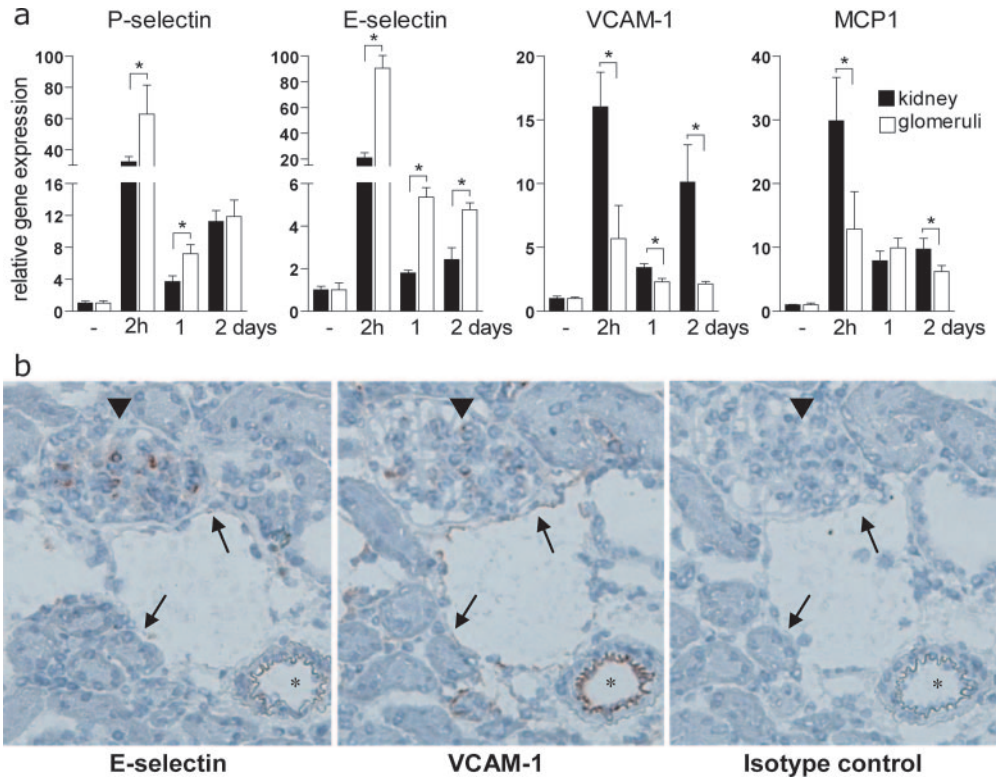

Fig. 3. Glomerular up-regulation of cell adhesion molecules after induction of glomerulonephritis. a, up-regulation of P- and E-selectin, VCAM-1, and MCP1 in microdissected glomeruli and total kidney isolates at 2 h, 1 day, and 2 days after glomerulonephritis induction. Expression levels of mRNA in untreated mice (−) were arbitrarily set at one for total kidney isolates and microdissected glomeruli, respectively. Data are presented as mean values ± S.E.M. of six animals per treatment. *, $p < 0.05$ up-regulation in glomeruli compared with whole-kidney isolates. b, immunohistochemical staining with anti-E-selectin antibodies, anti-VCAM-1 antibodies, and isotype-matched control antibodies at 2 h after glomerulonephritis induction. Asterisk, arteriole; arrowhead, glomerulus; arrow, venule.

time points. Similar to up-regulation of VCAM-1, glomerulonephritis-induced expression of MCP1 was predominantly located outside the glomeruli (Fig. 3a).

Gene expression data were corroborated by immunohistochemical analysis for E-selectin and VCAM-1 (Fig. 3b). E-selectin protein was solely produced in glomeruli, whereas VCAM-1 was present in glomerular capillaries and in microvascular beds outside the glomeruli. The immunostaining of VCAM-1 was weak in glomeruli and stronger in arterioles. Althought E-selectin protein was undetectable in untreated mice, 2 h after disease induction 75 ± 5% of all glomeruli were positive for E-selectin. After 2 days, the presence of glomerular E-selectin expression was decreased to 39 ± 13% of all glomeruli.

I.V. Administered Ab_{Esel}-Liposomes Selectively Homed to Glomeruli. The disease specific glomerular expression of E-selectin provided it a promising target molecule on glomerular endothelial cells. Immunohistochemical staining demonstrated selective homing of i.v. administered immunoliposomes containing monoclonal anti-E-selectin antibodies (Ab_{Esel}) to the diseased glomeruli (Fig. 4a). No staining was observed elsewhere in the kidney. This localization remained during disease development, although in time the staining became less pronounced. Glomerular staining of Ab_{Esel} liposomes was detected at 2 h in 93 ± 4%, at 1 day in 90 ± 1%, and at 2 days in 81 ± 6% of all glomeruli; approximately 10% of the glomerular surface was positive for the specific immunoliposome (Fig. 4b). Control IgG liposomes localized in glomeruli, probably as a result of local inflammation-associated vascular permeability increase, but to a much lower extent (Fig. 4, a and b). No Ab_{Esel} liposomes localized in the heart, whereas some association of Ab_{Esel} liposomes was detected with cells in the red pulp in the spleen and with Kupffer cells in the liver, which reflects the regular elimination route of immunoliposomes in the body (data not shown).

To rule out the possibility that detecting the immunoliposomes using secondary antibody does not represent the liposomes themselves, we applied in a parallel experiment, radioactive [^{3}H]cholesteryloleyl ether labeled Ab_{Esel} liposomes or IgG liposomes, and analyzed the kidney uptake of both liposome-preparations. The experiment demonstrated a targeting index of the lipid part of Ab_{Esel} liposomes/IgG liposomes of 3.6:1 (S. A. Ásgeirsdóttir, J. A. A. M. Kamps, unpublished results), which corresponded nicely to the glomerular surface staining by immunohistochemistry as shown in Fig. 4b.

Based on this selective homing to inflamed glomerular endothelium, Ab_{Esel} liposomes were next employed as carriers for a targeted delivery of dexamethasone to interfere with glomerular endothelial cell activation and hence to counteract glomerulonephritis development and progression.

Targeted Dexamethasone Exerted Strong, Local Pharmacological Effects without Alteration of Blood Glucose Level. Dexamethasone has pleiotropic anti-inflammatory effects, including an interaction with the transcription factors NF-κB and AP-1, thereby preventing expression of proinflammatory genes (Barnes, 2006). We therefore compared the effects of Ab_{Esel} liposomes encapsulated dexamethasone and free dexamethasone by analyzing mRNA levels of proinflammatory genes. As expected, none of the treatments prevented depositions of sheep and mouse immunoglobulin in glomeruli (data not shown). Kidneys were harvested after 2 h, a time point when proinflammatory genes were robustly up-regulated. Free dexamethasone significantly inhibited gene expression induction of cell adhesion molecules and cytokines (Fig. 5a). Targeted liposomal delivery of dexamethasone similarly resulted in significant down-regulation of P- and E-selectin, whereas cytokine expression was affected slightly but not statistically significantly. No effects on proinflammatory gene expression were observed in mice treated with empty Ab_{Esel} liposomes (Fig. 5a).

It is noteworthy that expression of VCAM-1 was inhibited by free dexamethasone but not by cell-selective delivery into glomerular endothelium. Based on our data on predominant nonglomerular expression of VCAM-1 (Fig. 3a), we hypothesized that this discrepancy was due to local pharmacological effects of Dexa-Ab_{Esel} liposomes in the glomeruli, combined

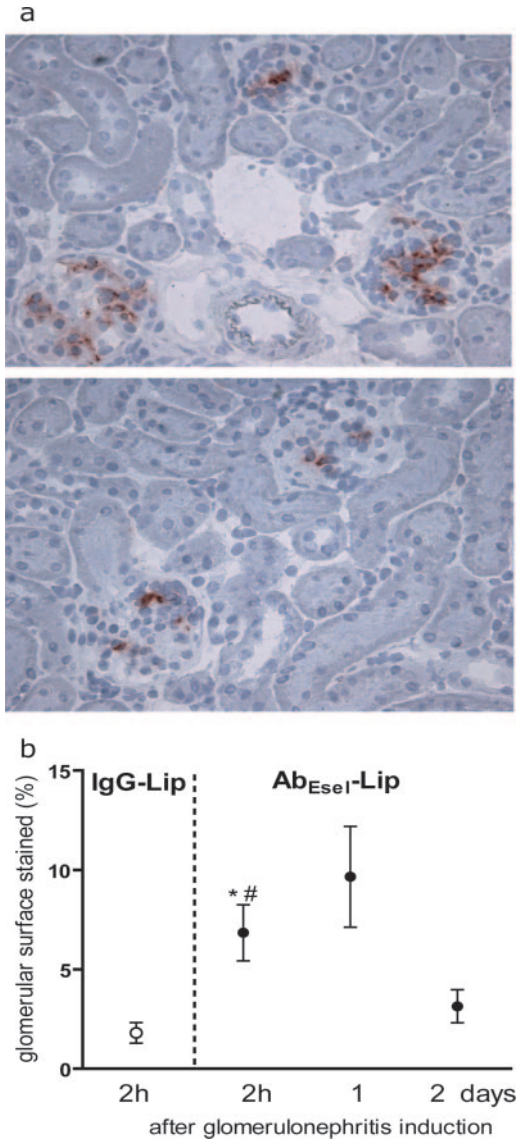

Fig. 4. Intravenously injected Ab_{Esel} liposomes selectively homed to glomeruli at the onset of glomerulonephritis. a, immunohistochemical detection of Ab_{Esel} liposomes (top) and control IgG liposomes (bottom) 2 h after glomerulonephritis induction. b, quantitative morphometric analysis of intraglomerular immunohistochemical staining of control IgG liposomes and Ab_{Esel} liposomes. Values indicate mean ± S.E.M. of three animals per treatment group. *, $p < 0.05$ compared with control Ig liposomes. #, no significant difference was observed between Ab_{Esel} liposomes at different time points.

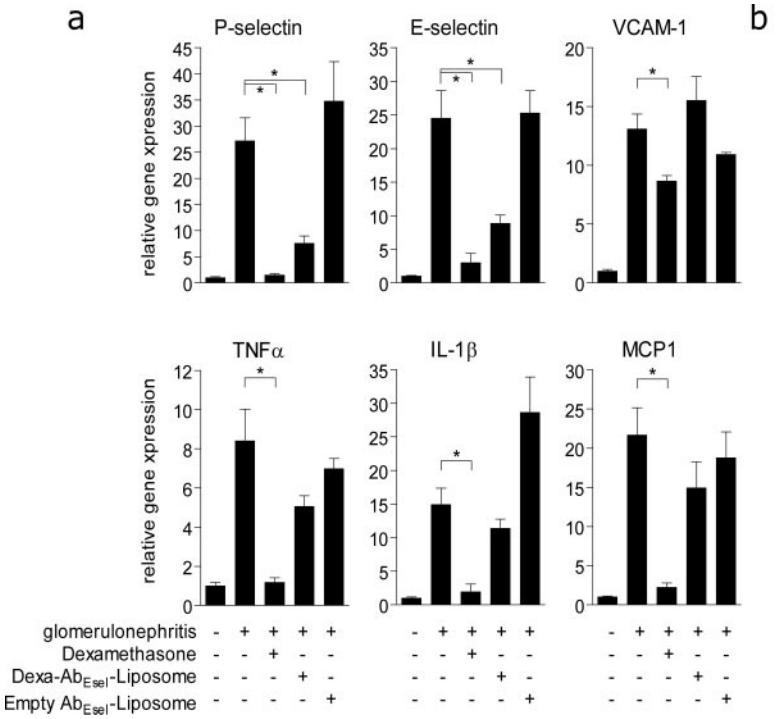

Fig. 5. Dexamethasone and Dexa-Ab$_{Esel}$ liposomes strongly down-regulated proinflammatory gene expression in glomerulonephritis. a, gene expression levels in whole-kidney isolates of untreated mice and 2 h after induction of glomerulonephritis in the absence or presence of dexamethasone, Dexa-Ab$_{Esel}$ liposomes and empty Ab$_{Esel}$ liposomes, respectively. Expression levels of mRNA in untreated mice were arbitrarily set at 1. Data are presented as mean values ± S.E.M. of 4 to 12 mice, *, $p < 0.05$. b, down-regulation of glomerular expression of VCAM-1 and MCP1 by Dexa-Ab$_{Esel}$ liposomes. RNA was isolated from microdissected glomeruli. Expression levels of mRNA in untreated mice (hatched bar) were arbitrarily set at one. Disease associated glomerular expression (black bar) of VCAM-1 and MCP1 was prevented by treatment with Dexa-Ab$_{Esel}$ liposomes (white bar). Data are presented as mean values ± S.E.M. of six mice. *, $p < 0.05$

with a relatively low expression of VCAM-1 therein. We therefore studied the effect of Dexa-Ab$_{Esel}$ liposome on the expression levels of VCAM-1 in microdissected glomeruli and demonstrated that glomerular expression of VCAM-1 was indeed down-regulated by Dexa-Ab$_{Esel}$ liposomes (Fig. 5b). Likewise, glomerular expression of MCP1 was down-regulated by Dexa-Ab$_{Esel}$ liposomes, whereas no effect on MCP1 expression was observed in whole-kidney isolates (Fig. 5). Down-regulation of P- and E-selectin in microdissected glomeruli was comparable with that observed in whole-kidney isolates (data not shown), corroborating the predominant expression of these cell adhesion molecules in glomeruli (Fig. 3a). Dexamethasone is known to cause many side effects, such as osteoporosis, growth retardation in children, skin fragility, and metabolic effects (Barnes, 2006). Hyperglycemia, caused by induction of hepatic gluconeogenesis and inhibition of cellular glucose uptake, is one of the earliest clinically relevant side effects of dexamethasone (Weinstein et al., 1995; Feldman-Billard et al., 2006; Hans et al., 2006).

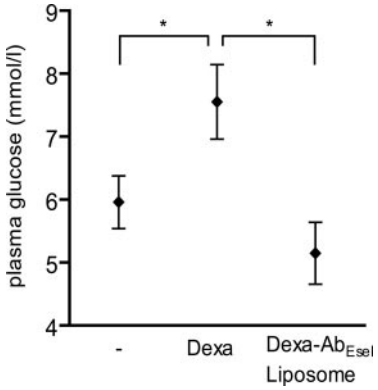

Fig. 6. Increased plasma glucose levels in mice treated with free dexamethasone; Dexa-Ab$_{Esel}$ liposomes were devoid of this systemic side effect. Control mice (−): 2-h glomerulonephritis induction without drug treatment. Values represent mean ± S.E.M. of 6 to 12 mice. *, $p < 0.05$.

Indeed, in mice treated with free dexamethasone, the plasma glucose concentration 2 h after i.v. injection of the drug was significantly increased (Fig. 6). This was not observed in mice i.v. injected with dexamethasone encapsulated in immunoliposomes (Fig. 6).

Treatment with Dexa-Ab$_{Esel}$ Liposomes Ameliorates Glomerulonephritis Progression. To study whether targeted inhibition of inflammatory gene expression in glomeruli would be able to counteract the occurrence of renal injury during glomerulonephritis development, mice were treated at days 0 and 7 with free dexamethasone, Dexa-Ab$_{Esel}$ liposomes, or empty Ab$_{Esel}$ liposomes and sacrificed at day 14.

Plasma BUN levels in mice treated with Dexa-Ab$_{Esel}$ liposomes were decreased compared with levels in mice treated with Ab$_{Esel}$ liposomes (Fig. 7a). A similar reduction in BUN levels was observed in mice treated with free dexamethasone. A trend toward improved glomerular function exemplified by increased creatinine clearance was observed in both Dexa-Ab$_{Esel}$ liposomes and dexamethasone-treated mice (Fig. 7b). Moreover, Dexa-Ab$_{Esel}$ liposomes were able to strongly inhibit the formation of crescents in glomeruli (Fig. 7, c and d). The percentages of crescentic glomeruli decreased significantly from 30 ± 4% to 17 ± 4% (mean ± S.E.M.). Free dexamethasone showed a similar trend but with a greater variation between mice (Fig. 7c). Overall, renal injury was notably counteracted by treatment with Dexa-Ab$_{Esel}$ liposomes, demonstrated by less glomerular lesions, intratubular protein casts, and tubulointerstitial damage (Fig. 7d). Control Dexa-IgG liposomes, which did end up in the kidney to a 4-fold lower extent than targeted Dexa-Ab$_{Esel}$ liposomes (see Fig. 4b), did reduce BUN levels to 13.4 ± 2.4 (mean ± S.E.M), a pharmacological effect that is most probably associated with inflammation-related enhanced permeability and retention-based passive accumulation and subsequent local

slow drug release. In contrast, these nontargeted liposomes did not result in reduction of the formation of crescentic glomeruli (29 ± 3%; mean ± S.E.M.) or in improvement of creatinine clearance.

Concomitantly with improved renal function, treatment with Dexa-Ab_{Esel} liposomes decreased the expression of disease-related inflammatory genes at day 14. Expression levels of VCAM-1 and fibrosis-related TGFβ were markedly lower in mice receiving Dexa-Ab_{Esel} liposomes compared with empty Ab_{Esel} liposomes (Fig. 8). Likewise, a significant reduction in MCP1 and IL-6 mRNA levels was observed, whereas a trend toward down-regulation of IL-1β and TNFα was detected. Administration of free dexamethasone resulted in significant down-regulation of VCAM-1 and MCP1, whereas TGFβ, IL-6, IL-1β, and TNFα were not statistically significantly affected.

Discussion

In this study, we demonstrate that targeted delivery of dexamethasone into glomerular endothelium by liposomes, modified with E-selectin-specific monoclonal antibodies as a homing device, selectively inhibited proinflammatory gene expression and improved renal function in progressive glomerulonephritis. Furthermore, the selective glomerular delivery of dexamethasone prevented unwanted systemic side effects that were observed after administration of free dexamethasone.

Anti-GBM crescentic glomerulonephritis can be treated with immunotherapy (Tam, 2006). Nonetheless, the need for more specific therapies is evident. The functional redundancy of molecules involved in leukocyte-endothelial cell interactions, as well as the complexity of inflammatory

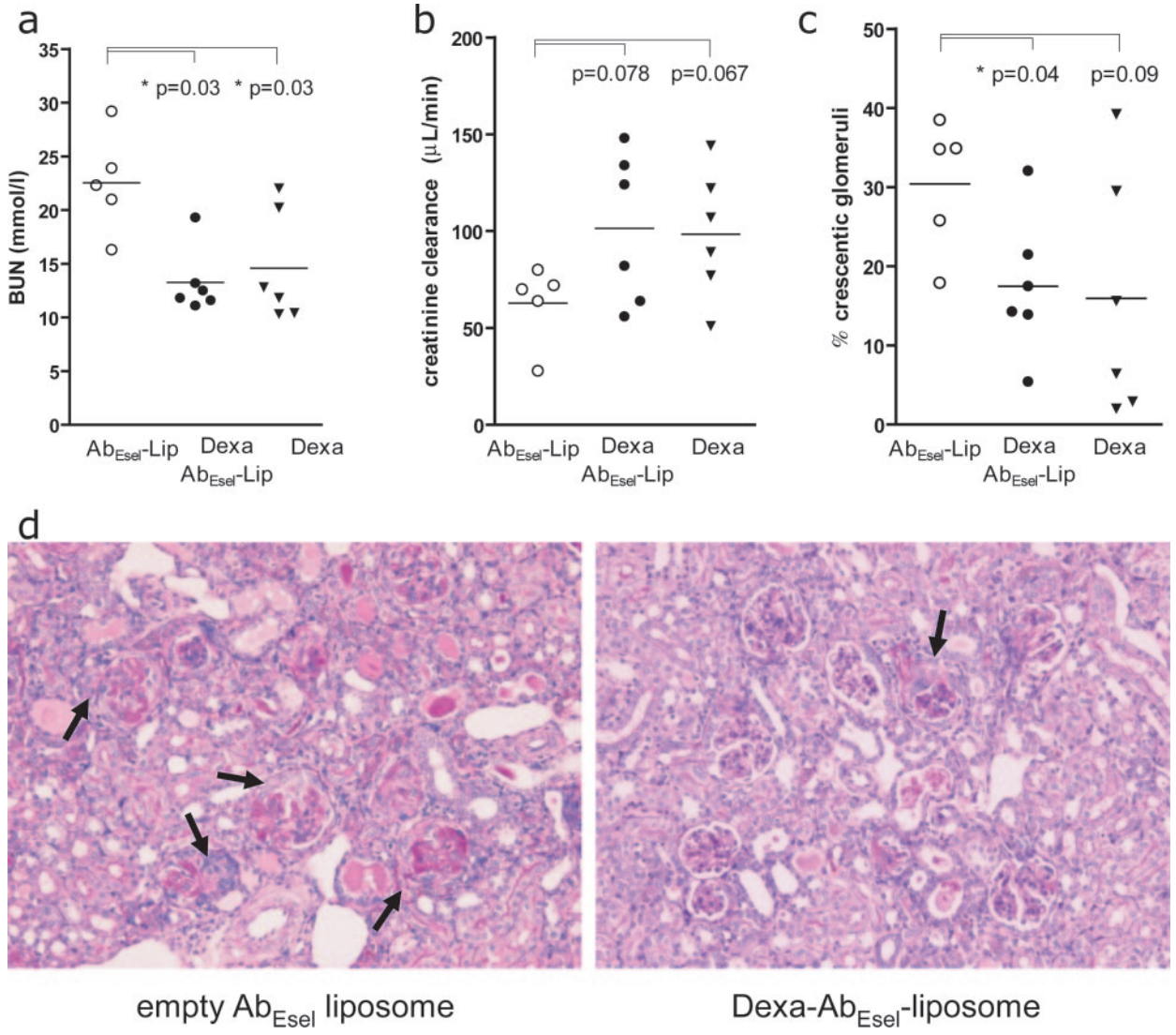

Fig. 7. Selective delivery of dexamethasone into glomerular endothelial cells reduced renal injury during progression of glomerulonephritis. Mice were i.v. injected at days 0 and 7 with empty Ab_{Esel} liposomes (○), Dexa-Ab_{Esel} liposomes (●) and free dexamethasone (▼). a, plasma BUN levels at day 14 after glomerulonephritis induction were reduced in mice treated with Dexa-Ab_{Esel} liposomes and dexamethasone. b, a trend toward increased creatinine clearance at day 14 after glomerulonephritis induction was observed in mice treated with Dexa-Ab_{Esel} liposomes and dexamethasone. c, glomerular crescent formation at day 14 after glomerulonephritis induction was significantly reduced in mice treated with Dexa-Ab_{Esel} liposomes. d, representative PAS staining of kidney induction from mice treated with empty Ab_{Esel} liposomes (left) and Dexa-Ab_{Esel} liposomes (right) at day 14 after glomerulonephritis. The frequency of glomerular crescent formation (arrows), intratubular protein casts, and tubulointerstitial injury were reduced in the Dexa-Ab_{Esel} liposome treated mice.

gene expression control and protein function, justifies cell-specific therapeutic intervention with a broad pharmacological spectrum (Rosenkranz and Mayadas, 1999; Kuldo et al., 2005). Therefore, we postulated that selective delivery of a potent anti-inflammatory drug with pleiotropic pharmacological effects into glomerular endothelium could

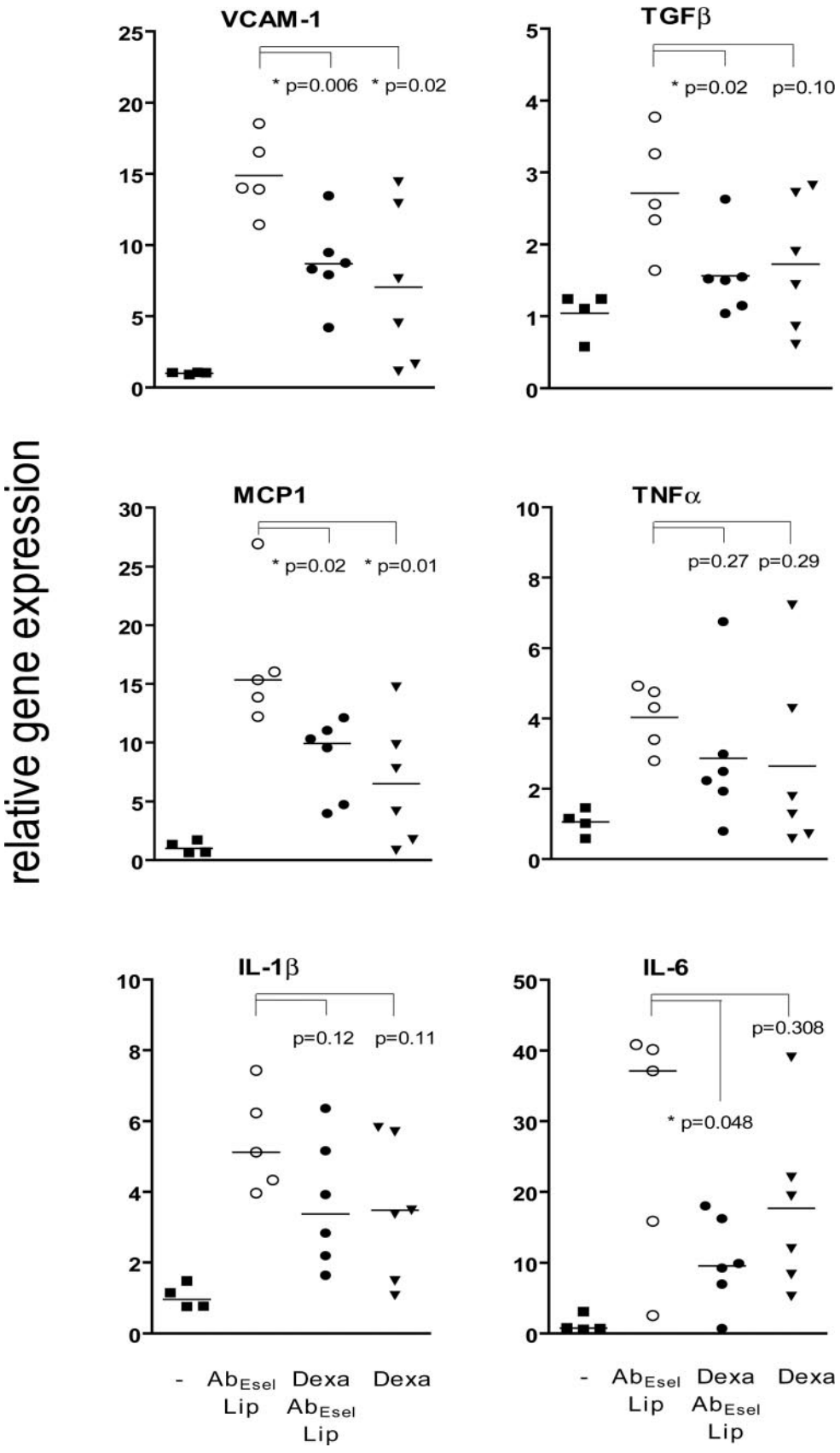

Fig. 8. Targeting dexamethasone to glomerular endothelium reduced expression of proinflammatory genes during progression of glomerulonephritis. Mice were i.v. injected at days 0 and 7 of glomerulonephritis development with empty Ab_{Esel} liposomes (○), Dexa-Ab_{Esel} liposomes (●) and free dexamethasone (▼). Gene expression was analyzed in whole-kidney isolates at day 14. Expression levels of mRNA in healthy control mice (■) were arbitrarily set at 1.

exert a broad, yet local, inhibitory effect but prevent systemic side effects.

The current study is the first report describing a successful targeted delivery of drug-loaded immunoliposomes to activated glomerular endothelial cells in glomerulonephritis in which local pharmacological activity did not interfere with vascular integrity. The local and disease-specific expression of E-selectin on glomerular endothelium rendered it an excellent target molecule for drug delivery-based therapy in glomerulonephritis. We have reported a rapid receptor-mediated internalization of anti E-selectin drug conjugates via E-selectin on activated endothelial cells (Kok et al., 2002; Asgeirsdottir et al., 2003; Everts et al., 2003). This intracellular delivery allows endothelial cell-specific pharmacological interference of regulatory mechanisms to control and inhibit the expression of proinflammatory mediators such as cytokines and adhesion molecules, as demonstrated by our current data.

The fact that elevated E-selectin expression has been detected in the kidney of patients with IgA nephropathy, lupus nephritis, and diabetic nephropathy supports the clinical relevance of the development of E-selectin-based drug-targeting strategies (Hirata et al., 1998; Honkanen et al., 1998). The use of endothelial target epitopes other than E-selectin, however, can be taken into account. Immunoliposomes directed toward VCAM-1 were internalized by activated endothelial cells in vitro (Voinea et al., 2005) and, in vivo, demonstrated beneficial effects in an atherosclerosis mouse model (Homem de Bittencourt et al., 2007). The use of VCAM-1-selective immunoliposomes in glomerulonephritis to interfere with microvascular endothelial cells distinct from the glomerular capillaries is an attractive strategy, especially because VCAM-1 is highly expressed throughout disease progression (Allen et al., 1999).

Laser capture microdissection is a valuable tool in (patho)-physiology research because it allows, in combination with qRT-PCR, the detection of local disease activity that would otherwise be masked in analysis of a whole organ. For drug delivery research, microdissection is also instrumental in revealing local molecular targets of the therapeutic strategy studied. Using this approach, we demonstrated that in our glomerulonephritis model, up-regulation of proinflammatory genes differed between the microvascular beds in the kidney. Strong up-regulation of E-selectin was observed on glomerular endothelium, whereas VCAM-1 and MCP1 expression was mainly localized outside the glomeruli. Furthermore, RNA isolates of microdissected glomeruli revealed local down-regulation of VCAM-1 and MCP1 by Dexa-Ab_{Esel} liposomes, whereas the expression levels of these genes in whole kidney isolates were not altered. It is clear that analysis in whole-kidney isolates would lead to wrong conclusions about the pharmacological efficacy of Dexa-Ab_{Esel} liposomes.

Targeted delivery to glomerular endothelium resulted in strong local pharmacological effects. In our study, we used dexamethasone, a corticosteroid that is generally well tolerated after systemic administration, as a model drug to demonstrate proof of concept. However, many potent anti-inflammatory drugs do not make it through clinical trials today because of severe side effects (Peifer et al., 2006). For these classes of drugs, the targeted delivery approach described in this study represents an important added value for future clinical applications. The challenge for the future drug delivery will be to formulate new chemical entities that are rapidly being discovered and are currently making their ways into basic research and clinical trials. These new drugs include tyrosine kinase inhibitors, mitogen-activated protein kinase inhibitors, and other agents interfering with proinflammatory signal transduction pathways (Bergers et al., 2003; Fabian et al., 2005; Karin, 2006). The recent observation that their molecular targets are fundamental in whole-body homeostasis makes their incorporation into cell-type–specific drug delivery systems of essential value for clinical utility (Imming et al., 2006).

We showed that Dexa-Ab_{Esel} liposomes were highly effective in improving renal function in glomerulonephritis, as reflected by reduced BUN levels, glomerular crescent formation, and proinflammatory gene expression. Although free dexamethasone was also effective, encapsulation of dexamethasone into immunoliposomes prevented the occurrence of the increased plasma glucose levels observed after administration of free dexamethasone. Hence, immunoliposomal delivery of potent drugs into inflamed microvascular endothelium maintains the pharmacological quality of the drug but eliminates systemic side effects and, as such, represents a new therapeutic strategy for the treatment of glomerulonephritis.

Acknowledgments

We thank Dr. D. Brown for providing MES-1 antibodies, Pieter A. Klok for assistance in animal experiments, Dr. Eniko Sajti for valuable discussions regarding systemic side effects of dexamethasone, and Dr. Joanna Adrian for advice regarding calculation of the number of antibodies per liposome.

References

Adrian JE, Kamps JA, Scherphof GL, Meijer DK, van Loenen-Weemaes A, Reker-Smit C, Terpstra P and Poelstra K (2007) A novel lipid-based drug carrier targeted to the non-parenchymal cells, including hepatic stellate cells, in the fibrotic livers of bile duct ligated rats. *BBA Biomembranes*, in press.

Allen AR, McHale J, Smith J, Cook HT, Karkar A, Haskard DO, Lobb RR, and Pusey CD (1999) Endothelial expression of VCAM-1 in experimental crescentic nephritis and effect of antibodies to very late antigen-4 or VCAM-1 on glomerular injury. *J Immunol* **162:**5519–5527.

Asgeirsdóttir SA, Kok RJ, Everts M, Meijer DK, and Molema G (2003) Delivery of pharmacologically active dexamethasone into activated endothelial cells by dexamethasone-anti-E-selectin immunoconjugate. *Biochem Pharmacol* **65:**1729–1739.

Assmann KJ, Tangelder MM, Lange WP, Schrijver G, and Koene RA (1985) Anti-GBM nephritis in the mouse: severe proteinuria in the heterologous phase. *Virchows Arch A Pathol Anat Histopathol* **406:**285–299.

Barnes PJ (2006) How corticosteroids control inflammation: quintiles prize lecture 2005. *Br J Pharmacol* **148:**245–254.

Bartsch M, Weeke-Klimp AH, Meijer DK, Scherphof GL, and Kamps JA (2005) Cell-specific targeting of lipid-based carriers for ODN and DNA. *J Liposome Res* **15:**59–92.

Bergers G, Song S, Meyer-Morse N, Bergsland E, and Hanahan D (2003) Benefits of targeting both pericytes and endothelial cells in the tumor vasculature with kinase inhibitors. *J Clin Invest* **111:**1287–1295.

Border WA and Noble NA (1994) Transforming growth factor beta in tissue fibrosis. *N Engl J Med* **331:**1286–1292.

Bottcher CDF, Van Gent CM, and Pries C (1961) Rapid and sensitive submicro phosphorus determination. *Anal Chim Acta* **24:**203–204.

Chadban SJ and Atkins RC (2005) Glomerulonephritis. *Lancet* **365:**1797–1806.

Enoch HG and Strittmatter P (1979) Formation and properties of 1000-Å-diameter, single-bilayer phospholipid vesicles. *Proc Natl Acad Sci U S A* **76:**145–149.

Eremina V, Sood M, Haigh J, Nagy A, Lajoie G, Ferrara N, Gerber HP, Kikkawa Y, Miner JH, and Quaggin SE (2003) Glomerular-specific alterations of VEGF-A expression lead to distinct congenital and acquired renal diseases. *J Clin Invest* **111:**707–716.

Everts M, Koning GA, Kok RJ, Asgeirsdottir SA, Vestweber D, Meijer DK, Storm G, and Molema G (2003) In vitro cellular handling and in vivo targeting of E-selectin-directed immunoconjugates and immunoliposomes used for drug delivery to inflamed endothelium. *Pharm Res* **20:**64–72.

Fabian MA, Biggs WH, III, Treiber DK, Atteridge CE, Azimioara MD, Benedetti MG, Carter TA, Ciceri P, Edeen PT, et al. (2005) A small molecule-kinase interaction map for clinical kinase inhibitors. *Nat Biotechnol* **23:**329–336.

Falk RJ, Jenette JC and Nachmann PH (2004) Primary glomerular disease, in *The Kidney* (Brenner BM ed) pp 1293–1380, W.B. Saunders, Philadelphia

Feldman-Billard S, Du Pasquier-Fediaevsky L, and Heron E (2006) Hyperglycemia

after repeated periocular dexamethasone injections in patients with diabetes. *Ophthalmology* **113:**1720–1723.
Hans P, Vanthuyne A, Dewandre PY, Brichant JF, and Bonhomme V (2006) Blood glucose concentration profile after 10 mg dexamethasone in non-diabetic and type 2 diabetic patients undergoing abdominal surgery. *Br J Anaesth* **97:**164–170.
Heeringa P, Van Goor H, Itoh-Lindstrom Y, Maeda N, Falk RJ, Assmann KJ, Kallenberg CG, and Jennette JC (2000) Lack of endothelial nitric oxide synthase aggravates murine accelerated anti-glomerular basement membrane glomerulonephritis. *Am J Pathol* **156:**879–888.
Hirata K, Shikata K, Matsuda M, Akiyama K, Sugimoto H, Kushiro M, and Makino H (1998) Increased expression of selectins in kidneys of patients with diabetic nephropathy. *Diabetologia* **41:**185–192.
Homem de Bittencourt PI Jr, Lagranha DJ, Maslinkiewicz A, Senna SM, Tavares AM, Baldissera LP, Janner DR, Peralta JS, Bock PM, Gutierrez LL, et al. (2007) Lipocardium: endothelium-directed cyclopentenone prostaglandin-based liposome formulation that completely reverses atherosclerotic lesions. *Atherosclerosis*, in press.
Honkanen E, von Willebrand E, Teppo AM, Tornroth T, and Gronhagen-Riska C (1998) Adhesion molecules and urinary tumor necrosis factor-alpha in idiopathic membranous glomerulonephritis. *Kidney Int* **53:**909–917.
Imming P, Sinning C, and Meyer A (2006) Drugs, their targets and the nature and number of drug targets. *Nat Rev Drug Discov* **5:**821–834.
Javaid B and Quigg RJ (2005) Treatment of glomerulonephritis: will we ever have options other than steroids and cytotoxics? *Kidney Int* **67:**1692–1703.
Kamps JA and Molema G (2006) Targeting liposomes to endothelial cells in inflammatory diseases, in *Liposome Technology, Volume III: Interactions of Liposomes with the Biological Milieu* (Gregoriadis G ed) pp 127–150, CRC Press.
Kamps JAAM, Morselt HWM, Swart PJ, Meijer DKF, and Scherphof GL (1997) Massive targeting of liposomes, surface-modified with anionized albumins, to hepatic endothelial cells. *Proc Natl Acad Sci U S A* **94:**11681–11685.
Kamps JAAM, Swart PJ, Morselt HWM, Pauwels R, de Béthune M-P, De Clercq E, Meijer DKF, and Scherphof GL (1996) Preparation and characterization of conjugates of (modified) human serum albumin and liposomes: drug carriers with an intrinsic anti-HIV activity. *Bba-Biomembranes* **1278:**183–190.
Karin M (2006) Nuclear factor-kappaB in cancer development and progression. *Nature* **441:**431–436.
Keppler A, Gretz N, Schmidt R, Kloetzer HM, Groene HJ, Lelongt B, Meyer M, Sadick M, and Pill J (2007) Plasma creatinine determination in mice and rats: an enzymatic method compares favorably with a high-performance liquid chromatography assay. *Kidney Int* **71:**74–78.
Kok RJ, Everts M, Asgeirsdottir SA, Meijer DK, and Molema G (2002) Cellular handling of a dexamethasone-anti-E-selectin immunoconjugate by activated endothelial cells: comparison with free dexamethasone. *Pharm Res* **19:**1730–1735.
Kuldo JM, Ogawara KI, Werner N, Asgeirsdottir SA, Kamps JA, Kok RJ, and Molema G (2005) Molecular pathways of endothelial cell activation for (targeted) pharmacological intervention of chronic inflammatory diseases. *Curr Vasc Pharmacol* **3:**11–39.
Masaki T, Chow F, Nikolic-Paterson DJ, Atkins RC, and Tesch GH (2003) Heterogeneity of antigen expression explains controversy over glomerular macrophage accumulation in mouse glomerulonephritis. *Nephrol Dial Transplant* **18:**178–181.
Melgert BN, Olinga P, Jack VK, Molema G, Meijer DKF, and Poelstra K (2000) Dexamethasone coupled to albumin is selectively taken up by rat nonparenchymal liver cells and attenuates LPS-induced activation of hepatic cells. *J Hepatol* **32:**603–611.
Peifer C, Wagner G, and Laufer S (2006) New approaches to the treatment of inflammatory disorders small molecule inhibitors of p38 MAP kinase. *Curr Top Med Chem* **6:**113–149.
Peterson GL (1977) A simplification of the protein assay method of Lowry et al. which is more generally applicable. *Anal Biochem* **83:**346–356.
Rosenkranz AR and Mayadas TN (1999) Leukocyte-endothelial cell interactions—lessons from knockout mice. *Exp Nephrol* **7:**125–136.
Spragg DD, Alford DR, Greferath R, Larsen CE, Lee KD, Gurtner GC, Cybulsky MI, Tosi PF, Nicolau C, and Gimbrone MA (1997) Immunotargeting of liposomes to activated vascular endothelial cells: a strategy for site-selective delivery in the cardiovascular system. *Proc Natl Acad Sci U S A* **94:**8795–8800.
Tam FW (2006) Current pharmacotherapy for the treatment of crescentic glomerulonephritis. *Expert Opin Investig Drugs* **15:**1353–1369.
Ulbrich H, Eriksson EE, and Lindbom L (2003) Leukocyte and endothelial cell adhesion molecules as targets for therapeutic interventions in inflammatory disease. *Trends Pharmacol Sci* **24:**640–647.
Vestweber D (2002) Regulation of endothelial cell contacts during leukocyte extravasation. *Curr Op Cell Biol* **14:**587–593.
Voinea M, Manduteanu I, Dragomir E, Capraru M, and Simionescu M (2005) Immunoliposomes directed toward VCAM-1 interact specifically with activated endothelial cells—a potential tool for specific drug delivery. *Pharm Res* **22:**1906–1917.
Weinstein SP, Paquin T, Pritsker A, and Haber RS (1995) Glucocorticoid-induced insulin resistance: dexamethasone inhibits the activation of glucose transport in rat skeletal muscle by both insulin- and non-insulin-related stimuli. *Diabetes* **44:**441–445.

Address correspondence to: S. A. Ásgeirsdóttir, Department of Pathology and Laboratory Medicine, Medical Biology Section, Hanzeplein 1, 9713 GZ Groningen, The Netherlands. E-mail: s.a.asgeirsdottir@med.umcg.nl